Vibrational predissociation of ArCl2: Toward the determination of the potential energy surface of the B state

Kenneth C. Janda, Octavio Roncero, and Nadine Halberstadt

Citation: J. Chem. Phys. **105**, 5830 (1996); doi: 10.1063/1.472425
View online: http://dx.doi.org/10.1063/1.472425
View Table of Contents: http://jcp.aip.org/resource/1/JCPSA6/v105/i14
Published by the American Institute of Physics.

Vibrational predissociation of $ArCl_2$: Toward the determination of the potential energy surface of the *B* state

Kenneth C. Janda
Department of Chemistry and ISIS, University of California, Irvine, California 92715

Octavio Roncero
IMFF-CSIC Serrano 123, 28006 Madrid, Spain

Nadine Halberstadt
LCAR-IRSMC, Université Paul Sabatier et CNRS, 31062 Toulouse Cedex, France

(Received 29 May 1996; accepted 1 July 1996)

Accurate quantum mechanical calculations are carried out to test the sensitivity of the spectroscopy and dynamics of the ***B*** state of $ArCl_2$ to the steepness of the Morse term, α, of an atom–atom potential. It is discovered that the predissociation dynamics for this molecule are very complicated even in the $\Delta v=-1$ regime due to resonances in the continuum manifold of states. In both the $\Delta v=-1$ regime and the $\Delta v=-2$ regime the rate of vibrational predissociation and the product rotational distribution are extremely sensitive to the value chosen for α, but not in a regular way. For the $\Delta v=-2$ regime the variations can be attributed to spacings between resonances and the overlaps of the bright state wave functions with nearby dark states as expected from the intramolecular vibrational relaxation model. In the $\Delta v=-1$ regime, the variations are shown to originate from resonances in the $v-1$ continuum set of states. Although this makes it difficult to determine the value for α, a value of 1.8 $Å^{-1}$ is probably close to the true value. The most useful new data to determine the potential would be measurements of the lifetimes for as many vibrational levels as possible and rotational distributions for excitation to low vibrational levels of the ***B*** state.
 [S0021-9606(96)01138-5]

I. INTRODUCTION

Triatomic van der Waals molecules provide one of the most tractable examples for an analysis of the mechanism for intramolecular vibrational relaxation (IVR) in real systems. That IVR should occur in such simple molecules was first evident in the highly structured rotational distributions observed in the vibrational predissociation in $ArCl_2$.[1] Subsequent quantum calculations on a reasonable model potential showed that this IVR occurs in the sparse limit.[2] That is, for the $\Delta v=-2$ dissociation of $ArCl_2$ from the $v=11$ Cl_2 stretching level, the initially excited ''bright'' state first couples to a single dark state in the manifold of van der Waals levels associated with the Cl_2 $v=10$ level before coupling to the continuum associated with the $v=9$ level. This is illustrated in Fig. 1. Since the dark state corresponds to a highly excited van der Waals mode, its nodal pattern is very complicated and this produces the structured rotational distributions of the final products. A different dark level is active for each initial Cl_2 stretching level, so both the rate of predissociation and the product rotational distribution are different for each initial Cl_2 vibrational level. This contrasts with directly dissociating species such as $HeCl_2$[3] and $NeCl_2$[4] for which the rotational distributions are smooth, and only weakly dependent on the degree of initial excitation of the Cl_2 stretch. Another interesting finding for the $ArCl_2$ IVR mechanism[5] is that the coupling between the bright and dark states is strongly influenced by the component of rotational excitation about the $ArCl_2$ bond (given by the quantum number Ω in the exact quantum treatment and roughly corresponding to the symmetric top K quantum number in the perpendicular configuration) but the coupling is only weakly dependent on the total J value for a given value of Ω.

The dissociation dynamics of ArI_2 are similar to those of $ArCl_2$ except that the smaller I_2 vibrational frequency results in a $\Delta v=-3$ dissociation mechanism involving a succession of at least two dark intermediate states. This case has recently been analyzed by Gray and Roncero.[6,7] They find that the vibrational levels studied decay by coupling to a small number of doorway states in the $\Delta v=-1$ and -2 manifolds before dissociating via the product continuum. Thus although the overall density of dark states is quite high, only a few are important for coupling to the initial quasibound state and coherent resonances are expected for state selected excitation. Due to this effect, the vibrational predissociation rate constant oscillates strongly as a function of the initially excited I_2 vibrational level within the complex. This conclusion appears to be in contradiction to the experimental data of Burke and Klemperer,[8] who concluded that the vibrational predissociation rate constant increases monotonically as a function of the I_2 vibrational excitation. Roncero and Gray have recently concluded that, since the coupling to the dark states is strongly dependent on rotational quantum numbers, and since it is not possible to prepare a rotationally state selected initial population, the coherent resonances are washed out in the observed spectra. $ArCl_2$ may be a better candidate for observation of such coherent decay since the dark states are less densely spaced and since fewer rotational levels are populated at a given temperature.

Because IVR in $ArCl_2$ involves specific bright–dark

 0021-9606/96/105(14)/5830/12/$10.00

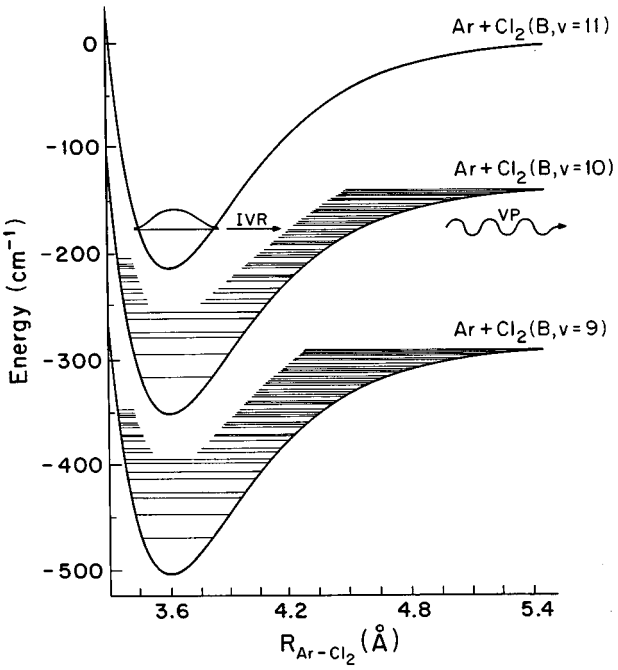

FIG. 1. Energy level scheme for IVR in $ArCl_2$. The zero order bright state corresponds to the ground van der Waals vibrational level associated with the $v=11$ level of the Cl_2 stretch. The doorway state is an excited van der Waals mode associated with the $v=10$ level of the Cl_2 stretch. The first open dissociation channel is for the $v=9$ level of the Cl_2 stretch. The complicated rotational distribution of the products is a result of the fact that the doorway state is highly excited in the van der Waals modes, and the complicated bending wave function has highly state-specific couplings to the rotational levels of the dissociation products.

resonances, which lead to highly specific rotational distributions, there is a prospect for a detailed fit of the Ar–Cl_2 potential. If the link between the dark state wave function and the product rotational distribution can be discovered, then the vibrational predissociation data would be roughly equivalent to having a van der Waals mode vibrational spectrum over a broad range of the van der Waals well. Unfortunately, such a link has not yet been discovered, and it is necessary to take a more incremental approach to determining the potential. Two key features of the potential already have been precisely determined. The dissociation energy of the $v=6$ level of the B state has been determined[1] to be 188 cm^{-1}, and the average Ar–Cl_2 bond length has been determined to be 3.7 Å for the B state[9] and 3.719 Å for the X state.[10] For any given potential form these measurements place narrow constraints on the value of the potential parameters. To completely determine the potential, it will be necessary to characterize the steepness, or width of the potential, and to learn more about the anisotropy of the potential parameters.

In this paper we explore the sensitivity of the IVR mechanism to the steepness of the potential. The $ArCl_2$ B state potential is expressed as a combination of atom-atom potentials as was done previously. Although it has recently been determined that the potential energy surfaces of the ground electronic states of rare gas–halogen van der Waals molecules are extremely anisotropic,[11,12] and not suitable for fitting to atom-datom potentials, the B state surfaces are probably very well described by such simple potentials. There are two reasons for this significant difference between the two electronic states. First, the intrahalogen bond in the B state is weak and long, so that the orbitals of the atoms are not too strongly perturbed by formation of the bond. Second, the electronic wave function for each halogen atom in the B state is best described as having an equal fraction of σ and π orbitals. This causes the anisotropy of the atoms to be averaged out. Here, we represent the short range part of the Ar–Cl potential, out to the inflection point of the well, with a Morse potential function. The steepness parameter, α, of the Morse function is varied over the range of 1.6 $Å^{-1} \leqslant \alpha \leqslant 2.0$ $Å^{-1}$ while the D_e and R_e(Ar–Cl) parameters are adjusted to yield the experimental D_0 and R_0 values. As might be expected, the IVR dynamics are extremely sensitive to the value of α, since it can shift dark states into and out of resonance with the bright state. A 10% change in the value of α can produce an almost 2 orders of magnitude change in the rate of vibrational predissociation in the IVR region. For $v=8$, the lowest level for which the $\Delta v=-1$ channel is closed and the molecule must dissociate via the $\Delta v=-2$ channel, there is a high density of dark states, but the coupling to them is relatively weak, on average. The expected lifetime is longer than 1 ns for the entire range of α parameters. For the higher vibrational levels, the coupling ranges from rather weak for $\alpha=1.6$ $Å^{-1}$ to very strong for $\alpha=2.0$ $Å^{-1}$. However, the trends are not monotonic since the coupling regime is sparse, even for the highest values of α.

The results for the low vibrational levels, which dissociate via the $\Delta v=-1$ channel, are quite surprising. Since the dynamics in this regime were expected to involve mainly direct coupling of the initially excited state to the dissociative continuum, we expected that the dissociation rate would scale monotonically with α, with larger values for α leading to stronger coupling and faster dissociation. This is not what was found. For instance, for the $v=7$ level, the calculated lifetime is 112 ps if $\alpha=1.92$ $Å^{-1}$ and 4600 ps if $\alpha=2.0$ $Å^{-1}$! This extreme sensitivity of the dissociation rate to the value of α is due to resonances of the initially excited state with continuum states whose wave functions have significant amplitude in the region of the van der Waals well. The resonances have the unusual effect of slowing down $\Delta v=-1$ dissociation, leading to a longer lifetime and enhanced $\Delta v=-2$ dissociation. Thus the dependence of the dissociation rate on α is not monotonic, even for vibrational levels for which the $\Delta v=-1$ channel is open. This effect has not previously been described for van der Waals molecule vibrational predissociation.

We conclude that the next step in determining an accurate $ArCl_2$ potential should be to measure the lifetimes of as many initial states of the complex as is possible. Although the lifetime of any one initial level could be due to a coincidental resonance, the average lifetime of a group of levels will help to define the strength of the coupling. It will also be useful to measure the $\Delta v=-2$ propensity in the $\Delta v=-1$ regime to determine the importance of coupling to reso-

nances in the continuum. Once the coupling strength is defined, then it may be possible to use the rotational distributions to infer information about the anisotropy of the potential.

II. METHODOLOGY

In this study we perform two types of calculations. First, the absorption spectra for $ArCl_2$ are calculated directly from the potential by integrating the coupled channel equations for the excited state. From these calculations we obtain the position, width and intensity for each resonance that has an appreciable Franck–Condon factor for excitation. This information serves as reference data for later analysis of the wave functions and dynamics. Rotational distributions are also obtained from the spectrum calculations by analyzing the scattering wave functions at large internuclear separation. The second type of calculation employs the ''golden rule'' approximation. The excited state resonances are analyzed as if they are quasibound states so that their nodal patterns and coupling can be separately analyzed. The golden rule calculations give us insight into the phenomena that are observed in the exact spectrum calculations.

The method used for these calculations and the form of the potential energy surface have been described in detail previously.[2] For the spectrum calculations the procedure can be briefly summarized as follows. A ground state wave function, which represents the molecule before laser excitation, is calculated using an appropriate bend–stretch basis set. The manifold of continuum states at the excitation energy are calculated by integration of rovibrational close-coupled equations with respect to the dissociative coordinate. The squared overlaps between the ground state wave function and the final state wave functions give the excitation intensity at each energy. By calculating the excitation cross section for a grid of excitation energies, the excitation spectrum is mapped out. The product vibrational–rotational distribution for each excitation energy is obtained from the partial cross sections.

The basis set needed to describe the excited state wave functions varies somewhat with the excitation energy and the coupling term of the potential surface. The results were always checked for convergence in both the size of the rovibronic basis and the integration length. Usually the spectrum was first calculated with a modest basis set size, and then the position and width of each resonance was recalculated with a large basis. A basis of six vibrational channels and 150 total rotational channels was usually adequate. For accurate final rotational distributions, it was necessary to integrate to 20 Å. The distribution of basis channels over the vibrational and rotational levels was similar to that described in our previous study of $ArCl_2$.[1]

The form used for the potential energy surface was also the same as that previously described. An atom–atom Morse potential describes the interaction of Ar with each Cl atom from the repulsive wall to the inflection point. Outside of the inflection point the potential is gradually switched to a van der Waals form. Our goal is to test the effect of varying the α parameter (the range factor). In our previous study this parameter was set at 1.8 $Å^{-1}$. Here, we investigate values ranging from 1.6 to 2.0 $Å^{-1}$. The well depth parameter was adjusted for each value of α in order to obtain the correct bond dissociation energy for the $v=6$ level of the B state. The R_e(Ar–Cl) parameter, the van der Waals parameters for the Ar–Cl interaction and the potential for the Cl–Cl interaction were not varied from the values previously used. A list of the potential parameters is given in Table I.

TABLE I. Parameters for the Morse part of the Ar–Cl potential[a] and the lowest bound state energy for $v=6$.

Potential number	$\alpha(Å^{-1})$	$D(cm^{-1})$	$E_0(cm^{-1})$
1	1.60	103.970	−178.24
2	1.70	104.974	−178.25
3	1.80	106.000	−178.29
4	1.86	106.620	−178.30
5	1.88	106.816	−178.28
6	1.90	107.022	−178.28
7	1.92	107.226	−178.28
8	2.00	108.078	−178.32

[a]In each case, R_e(Ar–Cl)=3.9 Å. The long range part of the potential is the same as in Ref. 2.

III. RESULTS

A. The $\Delta v=-1$ regime

When $ArCl_2$ is excited to the $v=5$, 6, or 7 levels of the Cl_2 stretch, the vibrational level spacings are such that the molecule can dissociate via a $\Delta v=-1$ channel. The total energy available for $\Delta v=-1$ dissociation for these three initial levels is 28 cm^{-1} for $v=5$, 18 cm^{-1} for $v=6$ and 7 cm^{-1} for $v=7$. We examine these levels first, because they are the ones that are expected to have the simplest behavior. Above $v=7$ the $\Delta v=-1$ channel is closed, and the results for those levels will be given below. For levels below $v=5$, the Franck–Condon factors for the transitions are very small, and there is no experimental data. Figure 2 shows a typical spectrum calculated for excitation to $v=7$, using the potential with $\alpha=1.8$ $Å^{-1}$. The resonance has a Lorentzian line shape, as expected. The width is 0.0079 cm^{-1} corresponding to a lifetime of 350 ps. This resonance decays mainly via the $\Delta v=-1$ channel, which accounts for 96% of the total decay probability.

The spectra calculated for other values of α also have Lorentzian line shapes, but the variation of the line width with α is not as simple as was expected. Since the α term in the Morse potential is the main coupling term between the Cl_2 stretch and the van der Waals modes, it is expected that the rate of vibrational predissociation should increase exponentially with α. For a simple system, one that obeys the ''energy gap law'' an expression $\ln(\Gamma)=-a(1/\alpha)+b$ holds,[13] where Γ is the dissociation rate. Figure 2 shows the dependence of Γ on α for the $ArCl_2$ spectrum calculations for $v=5$, 6, and 7. It is apparent from Fig. 3 that the real dependence of Γ on α is very complicated for these vibrational levels. The deviation from a monotonic dependence is

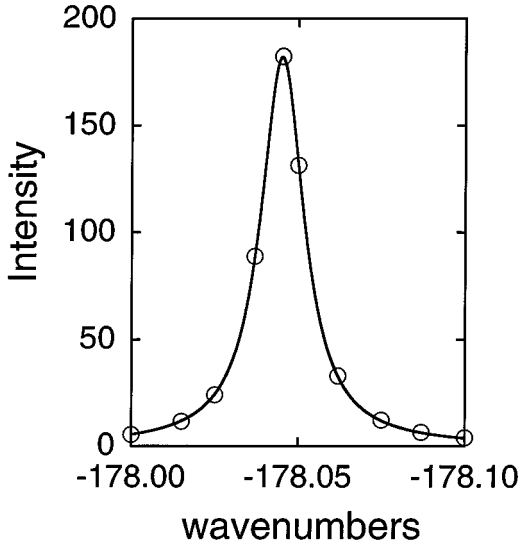

FIG. 2. The $J=0$ excitation spectrum to the $v=7$ level of $ArCl_2$ using $\alpha=1.8$ Å^{-1}. A Lorentzian line shape is obtained, as expected. The line width, 0.0079 cm^{-1}, corresponds to a lifetime of 350 ps. This level decays 96% via $\Delta v=-1$.

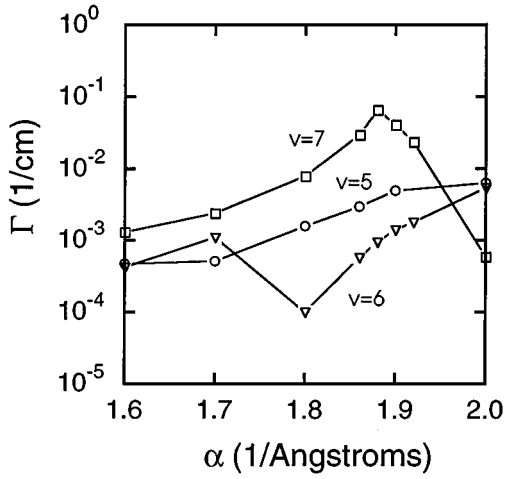

FIG. 3. The calculated dissociation rate (log scale) versus α parameter for the $v=5$, 6, and 7 levels of $ArCl_2$. The expected behavior was a monotonically increasing function. Instead, the effect of resonances with the continuum is to considerably reduce the rate for certain values of α.

largest for $v=7$, and appears to decrease for lower vibrational levels. This suggests that the unusual phenomena are related to the fact that the $\Delta v=-1$ channel is only slightly open for $v=7$, and somewhat more open for each lower vibrational level. Note that deviations from the expected trend tend to be toward very small values of Γ. That is, for certain values of α, the lifetime of the complex is much longer than expected from the energy gap law. For $v=7$, the lifetime decreases with α from 2 ns for $\alpha=1.6$ Å^{-1} to 41 ps for $\alpha=1.88$ Å^{-1}. For $\alpha=2.0$ Å^{-1}, which would have been expected to yield the shortest lifetime, the value is 4.6 ns.

The results of the spectrum calculations for the three vibrational levels as a function of α are summarized in Tables II, III, and IV. Note that α values that give small values of Γ also give a large probability for $\Delta v=-2$, which is otherwise only a minor dissociation channel. For each vibrational level, the anomalous behavior occurs for a different value of α. Another surprising result of the calculations is that the calculated rotational distributions are extremely sensitive to the value of α for each initial vibrational level. For instance, upon excitation to $v=5$, the average product rotational energy is 16.3 cm^{-1}, 57% of the total available kinetic energy for $\alpha=1.6$ Å^{-1}, but is only 3 cm^{-1}, 11% of the total for $\alpha=1.7$ Å^{-1}. This is in sharp contrast to the analogous results for $HeCl_2$,[3] $NeCl_2$,[4] HeICl,[14] and NeICl[15] for which the product rotational distributions are sensitive to the shape of the potential, but only slightly sensitive to the value of α or the initial vibrational level.

In the process of analyzing the resonances of the quasibound states with the background, we also carried out ''golden rule'' calculations of the bright state energy, lifetime, vibrational and rotational distributions for the $v=6$ and

TABLE II. $ArCl_2(v=5)$ Spectrum calculations and product probability distributions.[a]

α(Å^{-1})	1.6	1.7	1.8	1.86	1.9	2.0
E(cm^{-1})	−178.397 66	−178.427 156	−178.408 98	−178.512 36	−178.509 0	−178.574 24
Γ(cm^{-1})	0.000 467	0.000 507	0.001 59	0.002 973	0.004 96	0.006 34
τ(ps)	5850	5385	1717	918	550	430
% $v=2$	<.01	<.01	<.01	<.01	0.04	0.05
% $v=3$	0.4	0.6	0.8	1.1	1.8	3.1
% $v=4$	99.6	99.3	99.2	99.9	98.2	96.8
$v=4$, % $j=0$	2.0	25.1	14.3	14.1	14.2	12.7
$j=2$	1.6	27.5	20.1	10.9	4.1	8.8
$j=4$	0.7	22.2	16.4	7.1	4.2	18.5
$j=6$	4.3	16.1	20.1	22.1	21.3	5.7
$j=8$	32.6	4.9	13.4	16.2	13.1	2.9
$j=10$	19.6	2.7	9.4	18.4	30.6	28.8
$j=12$	38.9	0.7	5.5	10.2	10.8	19.4

[a]E_0 is the center of the resonance that corresponds to the van der Waals vibrational ground state for v(Cl–Cl)=5. The energy is relative to dissociation limit for the van der Waals bond. Γ is the half width, half maximum of the resonance, and τ is the corresponding life time. Subsequent rows give the percent population for the product vibrational channels, and the rotational distribution for the first vibrational channel.

TABLE III. $ArCl_2(v=6)$ Spectrum calculations and product probability distributions.[a]

$\alpha(\text{Å}^{-1})$	1.6	1.7	1.8	1.86	1.88	1.90	1.92	2.0
$E_0(\text{cm}^{-1})$	−178.241 1	−178.2475	−178.288 2	−178.299 1	−178.282 9	−178.2841	−178.2806	−178.3186
$\Gamma(\text{cm}^{-1})$[a]	0.000 42	0.0011	0.000 10	0.000 57	0.000 940	0.0014	0.0018	0.0054
τ(ps)	6500	2500	27000	4800	2900	2000	1500	500
% $v=3$	<0.01	0.02	0.3	0.08	0.03	0.02	0.03	0.06
$v=4$	0.9	1.8	17.7	5.3	2.9	2.3	2.7	3.4
$v=5$	99.2	98.2	82.0	94.6	97.1	97.7	97.3	96.6
$v=5$, % $j=0$	29.3	8.02	14.7	10.6	11.5	11.0	7.9	2.7
$j=2$	23.2	20.3	11.2	33.7	30.4	26.7	21.0	22.0
$j=4$	4.3	37.7	17.2	25.5	26.5	26.8	28.3	19.0
$j=6$	8.2	2.1	15.9	6.6	7.9	7.8	6.5	22.5
$j=8$	1.0	17.9	18.4	5.9	8.3	11.3	17.3	19.3
$j=10$	33.2	12.2	4.7	12.4	12.6	14.1	16.4	11.1

[a]See Table II for an explanation of the symbols.

7 levels. In spite of the complicated dependence of the resonance on the value of α, the golden rule calculations reproduce most of the qualitative features of the more accurate spectrum calculations. For the $v=6$ level the golden rule calculations are able to predict the energy of the quasibound state to within 0.05 cm^{-1} for each value of α. The trend of dependence of lifetime on α is predicted qualitatively correctly, although the individual values are off by 20% and 50% for values of α other than 1.8 Å^{-1}. For $\alpha=1.8$ Å^{-1}, which is strongly affected by the resonance with the continuum states, the lifetime predicted by the golden rule is a factor of 5 too small. Similarly, the vibrational and rotational distributions obtained by the golden rule calculations are qualitatively similar to the accurate ones for most values of α, while the differences are significantly greater for $\alpha=1.8$ Å^{-1}. Similar results are obtained for the $v=7$ level. We conclude that the golden rule calculations are sufficiently accurate to help interpret the more precise, but much more time consuming, spectrum calculations. Also, in an effort to fit the potential the golden rule calculations are sufficiently accurate to serve as tool for an initial rough fit before refining the results with the spectrum calculations.

B. The $\Delta v=-2$ regime

For initial vibrational levels above $v=7$ of the B state, the $ArCl_2$ molecule dissociates via an IVR mechanism involving the transfer of at least two quanta of vibration from the Cl_2 stretching mode. In two previous studies[2,5] we have characterized the IVR as occurring in the sparse limit for $\alpha=1.8$ Å^{-1}. This means that usually an initial vibrational level dissociates by coupling to a single doorway state in the $\Delta v=-1$ manifold before reaching the dissociative continuum. In this regime the dissociation dynamics are expected to be very sensitive to the potential since small changes in the potential can move doorway states into and out of resonance. One goal of this study is to characterize the dependence of the dynamics on the Morse α parameter in order to obtain a more accurate potential.

For each vibrational level $8\leqslant v\leqslant 12$, we calculated the spectrum for ± 3 cm^{-1} around the bright state resonance. These spectra are shown in Figs. 4–8, and the results are summarized in Table V. These figures show that the spectra are quite sensitive to both the initial vibrational level and to the value of α used in the calculation. For $v=8$, the density of potential doorway states is relatively high since the $v=8$ bright state is situated only 3 cm^{-1} below the $v=7$ van der Waals dissociation limit. However, the coupling for $v=8$ is relatively weak since the frequency of the Cl_2 vibration is very high compared to that of the van der Waals modes. The density of potential doorway states is lower for the $v=12$ bright state since this state is 40 cm^{-1} below the $v=11$ van der Waals dissociation limit. The coupling for $v=12$ is relatively strong because the Cl_2 frequency is lower and the amplitude of vibration is larger than for $v=8$. On average, the

TABLE IV. $ArCl_2(v=7)$ Spectrum calculations and product probability distributions.[a]

$\alpha(\text{Å}^{-1})$	1.6	1.7	1.8	1.86	1.88	1.90	1.92	2.00
$E_0(\text{cm}^{-1})$	−178.0669	−178.0512	−178.0451	−178.0450	−178.0344	−178.049	−178.0577	−178.045 5
$\Gamma(\text{cm}^{-1})$[a]	0.0013	0.0024	0.0079	0.030	0.066	0.041	0.0240	0.000 59
τ(ps)	2000	1100	350	90	41	67	110	4600
% $v=4$	0.01	0.02	0.06	0.1	0.2	0.2	0.4	1.3
$v=5$	1.7	1.7	3.8	5.4	5.9	7.3	11.9	30.5
$v=6$	98.3	98.3	96.1	94.5	93.9	92.5	87.8	68.2
$v=6$, % $j=0$	19.1	22.6	46.6	43.4	36.3	33.9	30.5	49.7
$j=2$	15.9	28.7	7.5	22.5	24.6	23.8	21.5	7.0
$j=4$	8.0	32.7	11.7	22.9	23.9	23.8	21.6	4.0
$j=6$	55.3	14.3	30.2	5.7	9.2	11.0	14.2	7.5

[a]See Table II for an explanation of the symbols.

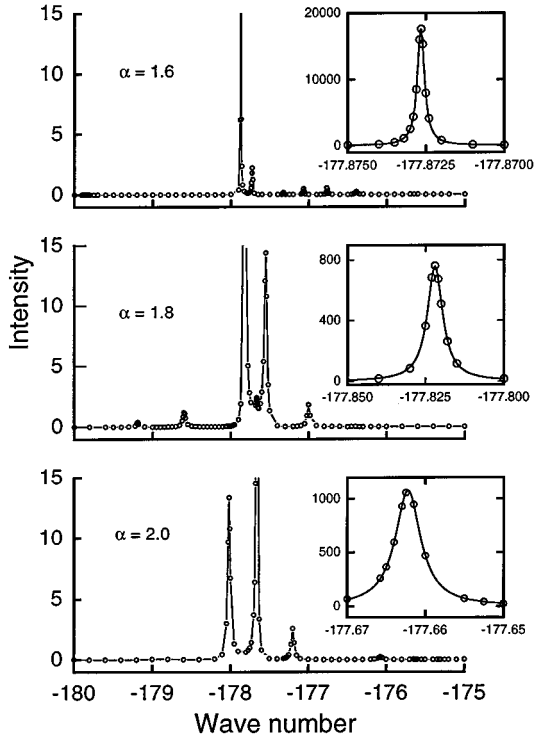

FIG. 4. The excitation spectrum in the region of the zero order bright state corresponding to $v=8$ of the Cl_2 stretch for α=1.6, 1.8, and 2.0 $Å^{-1}$. In this figure and the three following ones the whole spectrum is given at increased magnification for each value of α. The inset shows any resonances that are off scale in the main figure. Note that an indication of the coupling is the intensity of the bright state resonance. Weak coupling results in a narrow, intense resonance. The energy scale is relative to the dissociation limit of the zero order bright state. For this case, the dissociation rate is always relatively slow resulting in an intense, narrow bright state resonance. Notice that even the dark state resonances are fairly narrow. This is probably due to two effects. First, the vibrational amplitude is relatively small for $v=8$, so the coupling between the Cl_2 stretch and the van der Waals modes will be smaller than for higher vibrational levels. Second, the doorway states are high in the van der Waals manifold of states and therefore can not couple effectively to the dissociative continuum. Another effect of being high in the van der Waals continuum is that the dark state density is quite high, with six dark states at least slightly coupled to the bright state for α=1.6 $Å^{-1}$.

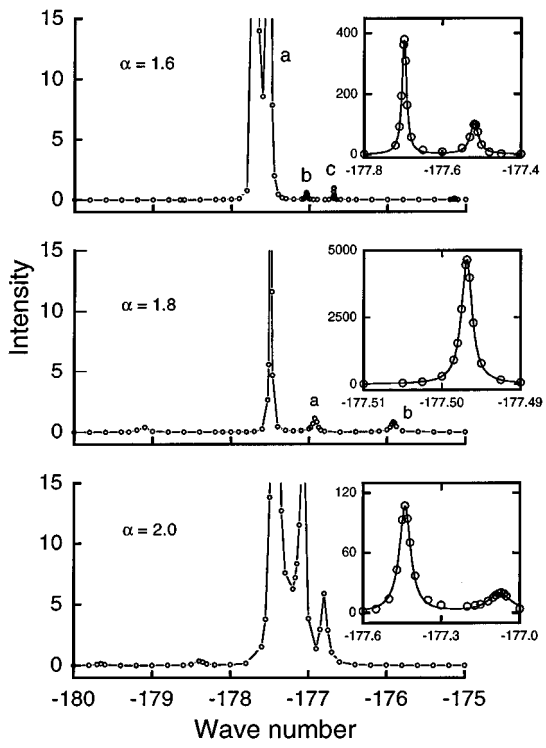

FIG. 5. The excitation spectrum in the region of the zero order bright state corresponding to $v=9$ of the Cl_2 stretch for α=1.6, 1.8 and 2.0 $Å^{-1}$. (See the caption of Fig. 4 for further explanation.) Here, α=1.6 $Å^{-1}$ results in strong coupling because of an accidental near degeneracy between the bright state and a doorway state. Wave functions for the dark states that induce the transitions marked *a*, *b*, and *c* are shown in Fig. 12. In contrast, α=1.8 $Å^{-1}$ results in weak coupling. Wave functions for the dark states that are marked *a* and *b* are shown in Fig. 13. Note that fewer dark states (compared to Fig. 4.) appear in the region of the calculation because the $v=9$ level is nested lower in the van der Waals manifold than the $v=8$ level.

expected trends are observed. That is, the coupling between bright and dark states increases with both the initial value of v and with α, and the number of dark states in the vicinity of the bright state decreases with v and with α. The spectra for $v=11$ are especially regular, as seen in Fig. 7. For α=1.6 $Å^{-1}$, the bright state is very narrow, with a 4.6 ns lifetime. Although five dark states are observed, the most strongly coupled dark state only accounts for 1% of the total intensity. For α=1.8 $Å^{-1}$, only two dark states are observed, but the coupling strength with the bright state is strong so that the bright state lifetime is only 290 ps, and the strongest dark state receives 15% of the total intensity. For α=2.0 $Å^{-1}$, two dark states are again observed, the bright state lifetime is down to 40 ps and the strongest dark state has 40% of the total intensity.

In contrast to the regular behavior for $v=11$, the $v=9$ spectra exhibit a very irregular dependence on α as shown in Fig. 5. The bright state lifetime is 390 ps, 3.3 ns, and 100 ps for α=1.6, 1.8, and 2.0 $Å^{-1}$, respectively. The resonance for α=1.6 $Å^{-1}$ is unusually broad because of an accidental near degeneracy between the bright state and a dark state. The resonance for α=1.8 $Å^{-1}$ is unusually narrow, since the bright state is only weakly coupled to the nearest dark state. This level is unusual in the sense that the bright state is about equally coupled to the nearest dark state, 0.57 cm^{-1} away, and the next nearest dark state, 1.6 cm^{-1} away. In order to more fully characterize the IVR behavior of each level as a function of v and α, Table V lists the transition frequency, integrated intensity, lifetime, fractional $\Delta v=-2$ decay, and the average product rotational energy for each bright state and the most strongly coupled dark states. The table also gives the correlation coefficient[16] between the product rotational distribution of the bright state with the most strongly coupled dark state. A value of the correlation coeffient near one indicates that the bright state dissociates primarily by coupling to a single doorway state.

Since the coupling between the bright state and the dark states is in the sparse regime, no monotonic trends are observed as a function of either the initially excited vibrational level or the assumed α parameter. The property that has the most regular behavior is the fraction of $\Delta v=-2$ decay.

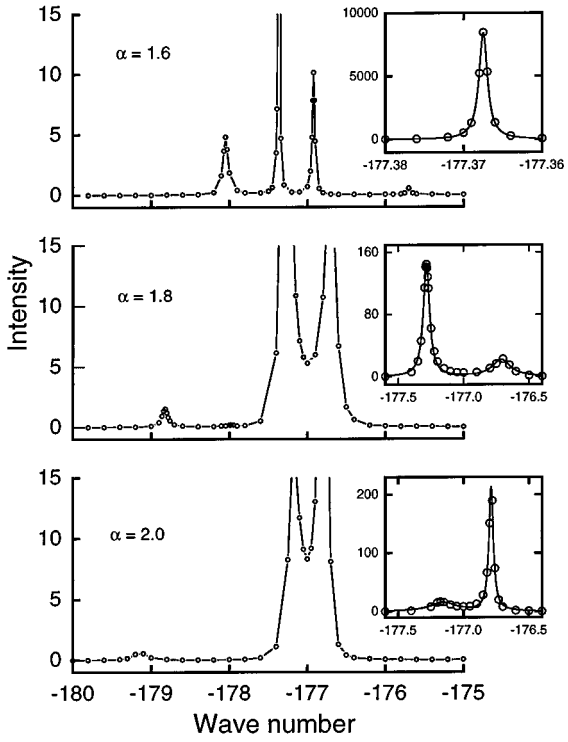

FIG. 6. The excitation spectrum in the region of the zero order bright state corresponding to $v=10$ of the Cl_2 stretch for α=1.6, 1.8, and 2.0 $Å^{-1}$. (See the caption of Fig. 4 for further explanation.) For this case the behavior is close to that expected in the sense that the coupling is weakest for α=1.6 $Å^{-1}$ and stronger for the other two values. Again, note the decrease in the number of dark states as v increases.

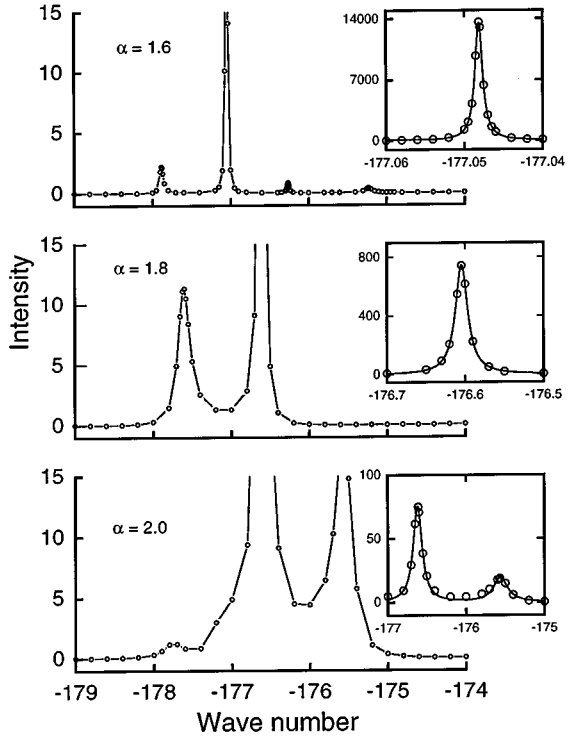

FIG. 7. The excitation spectrum in the region of the zero order bright state corresponding to $v=11$ of the Cl_2 stretch for α=1.6, 1.8, and 2.0 cm^{-1}. (See the caption of Fig. 4 for further explanation.) In this case the variation with v is as expected, with a monotonic increase in the coupling as α increases. This is probably due to the fact that the spacing between the bright state and the nearest dark state is approximately independent of the value of α, so that the value of α determines the coupling strength.

With a few exceptions this fraction generally decreases with increasing vibrational quantum number and with increasing α, as might have been expected. Figures 9 and 10 show the product rotational distributions for the $v=9$ and 10 initial vibrational levels as a function of the α parameter. The results for $v=10$ represent the expected behavior: in the weak coupling limit there is little correlation between the bright and dark state product rotational distributions. This is probably due to two complementary effects: First, the IVR coupling is weak due to the small value of α, and, second, there are two closely spaced doorway states coupled to the bright state. For α=1.8 and 2.0 $Å^{-1}$ the correlation between the rotational distribution of the bright state and the main doorway state is very high. This is expected since in both cases most of the IVR is due to a single doorway state strongly coupled to the bright state. The results for $v=9$ are less regular: for α=1.6 $Å^{-1}$, a near degeneracy results in strong correlation between the product rotational distributions. For α=1.8 and 2.0 $Å^{-1}$, there is no single dominant doorway state so the rotational distribution of the bright state is not similar to that of the strongest doorway state.

The calculated rotational distributions are very irregular for all vibrational levels and for all coupling strengths. In one case, $v=9$, α=2.0 $Å^{-1}$, 40% of the products go into the three lowest rotational channels; while for another case, $v=11$, α=1.6 $Å^{-1}$, only 5% of the products go into the lowest four channels and 50% of the product go into $J=16$, 18, and 20. On average, 26% of the available product kinetic energy (for the $\Delta v=-2$ channel) goes into the rotational degree of freedom, and the rest goes into translation. The fraction of the kinetic energy that goes into rotation appears to be roughly independent of the initial vibrational level, even when averaged over α, and appears to be inversely proportional to the value of α.

IV. DISCUSSION

A. The $\Delta v=-1$ regime

When $ArCl_2$ is excited to the $v=5$, 6 or 7 levels of the Cl_2 stretch, the molecule can dissociate via a $\Delta v=-1$ channel. Prior to this study, we would have invoked the energy gap law[13] to predict that the rate of vibrational predissociation would increase exponentially with the coupling parameter and with the vibrational level. However, Fig. 2 shows that the calculated dynamics are considerably more complicated than expected. For some values of α the lifetimes are much longer than expected from the energy gap law, and for these values of α there is also a surprisingly large probability for $\Delta v=-2$ decay. For instance, for the $v=6$ level, the lifetimes are 6.5 ns for α=1.6 $Å^{-1}$, 27 ns for α=1.8 $Å^{-1}$, and 0.5 ns for α=2.0 $Å^{-1}$. For these three values of α, the fraction of $\Delta v=-1$ decay is 99.2%, 82.0%, and 96.6%,

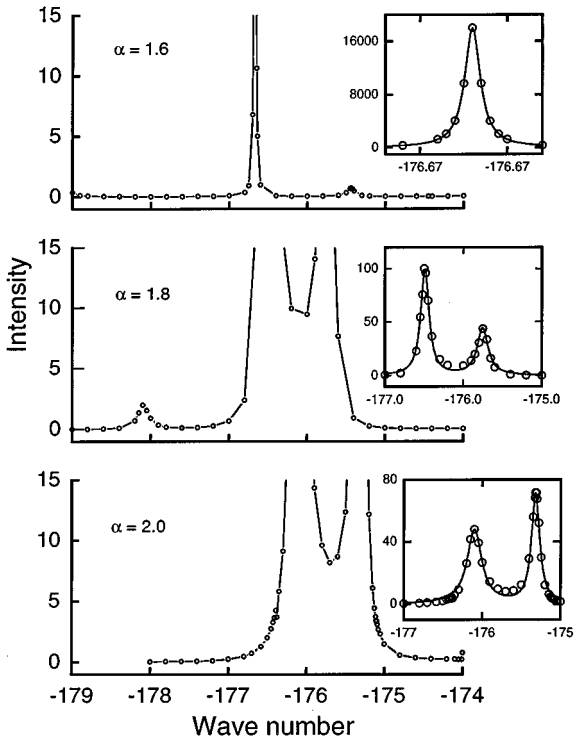

FIG. 8. The excitation spectrum in the region of the zero order bright state corresponding to $v=12$ of the Cl_2 stretch for α=1.6, 1.8, and 2.0 $Å^{-1}$. (See the caption of Fig. 4 for further explanation.) The density of dark states is down to about one for every three wave numbers. The coupling is quite weak for α=1.6 cm^{-1}. For the other two values of α the coupling is very strong.

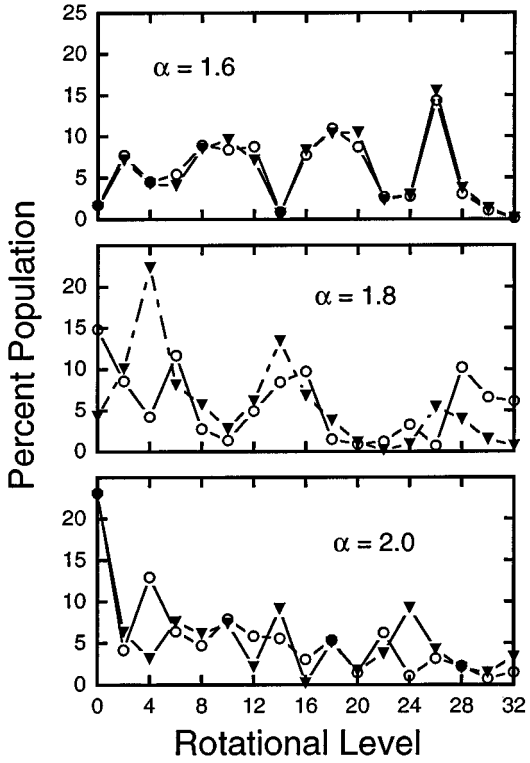

FIG. 9. The Cl_2 rotational distribution as a function of α for $\Delta v=-2$ dissociation of the zero order bright state and the most strongly coupled dark state is shown for initial excitation to $v=9$ of the Cl_2 stretch. To the extent that the dark state provides the principal dissociation doorway for the bright state, the two rotational distributions are quite similar. Here, this is seen to be the case for α=1.6 $Å^{-1}$. For $a=1.8$ $Å^{-1}$ the bright state is not coupled strongly to the nearest dark state for reasons discussed in the text. For α=2.0 $Å^{-1}$ a second dark state provides additional coupling so that the rotational distribution of the bright state is somewhat different from that of the main doorway state.

TABLE V. Results of the spectrum calculation for $ArCl_2$, $v=8$, 9, 10, 11, and 12.[a]

v	α ($Å^{-1}$)	τ_b (ps)	I_b	$\%\Delta v=-2$	$\langle E_{rot}\rangle$ (cm^{-1})	E_d-E_b (cm^{-1})	τ_d (ps)	I_d	Rot. Cor.[b]
8	1.6	19400	7.77	97.1	39.6	0.15	370	0.05	1.00
8	1.8	922	7.05	98.5	65.9	0.37	136	0.93	0.93
8	2.0	1385	6.67	96.7	48.8	0.36	151	0.7	0.88
9	1.6	384	8.41	96.5	43.6	0.18	210	4.18	0.76
9	1.8	3305	12.06	97.8	42.1	0.57	75	0.13	1.00
9	2.0	103	8.91	95.4	24.0	0.37	51	3.32	0.87
10	1.6	4200	17.18	95.1	24.2	0.68	74	0.57	0.99
10	1.8	94	13.30	98.5	38.8	0.58	33	5.90	0.41
10	2.0	130	13.30	95.6	29.6	0.29	37	4.00	1.00
11	1.6	4634	25.17	95.0	38.3	0.84	99	0.19	0.93
11	1.8	289	22.17	96.7	37.8	1.00	30	3.24	0.57
11	2.0	40	16.28	87.7	32.8	1.06	25	6.49	0.80
12	1.6	5062	30.50	92.1	14.9	3.02	33	0.80	0.95
12	1.8	42	20.15	95.7	35.3	0.74	32	11.64	0.75
12	2.0	42	16.80	87.9	21.8	0.78	24	13.90	0.92

[a]Explanation of column titles: v is the Cl_2 stretching quantum number of the zero order bright state. α is the Morse range parameter of the potential; τ_b is the bright state lifetime; I_b is the integrated intensity of the bright state resonance; $\%\Delta v=-2$ is the percent of the dissociation products found in the $\Delta v=-2$ channel; $\langle E_{rot}\rangle$ is the average rotational energy of the $\Delta v=-2$ dissociation channel; E_d-E_b is the splitting between the bright state resonance and the most intense dark state resonance; τ_d is the lifetime of the strongest dark state resonance; I_d is the integrated intensity of the strongest dark state resonance and the Rot. Cor. is the correlation coefficient between the rotational distributions of the bright state and the strongest dark state product rotational distributions.
[b]Reference 16.

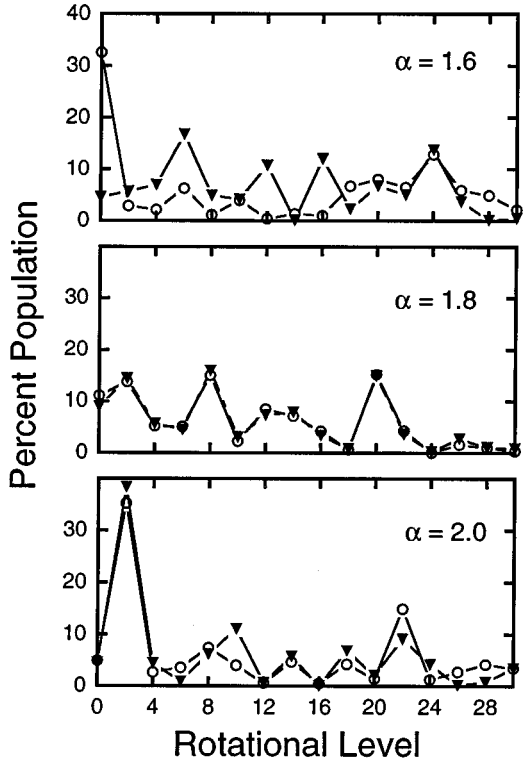

FIG. 10. The Cl_2 rotational distribution as a function of α for $\Delta v=-2$ dissociation of the zero order bright state and the most strongly coupled dark state is shown for initial excitation to $v=10$ of the Cl_2 stretch. To the extent that the dark state provides the principal dissociation doorway for the bright state, the two rotational distributions are quite similar. Here, this is the case for the two larger values of α, for which there is strong coupling to a single dark state.

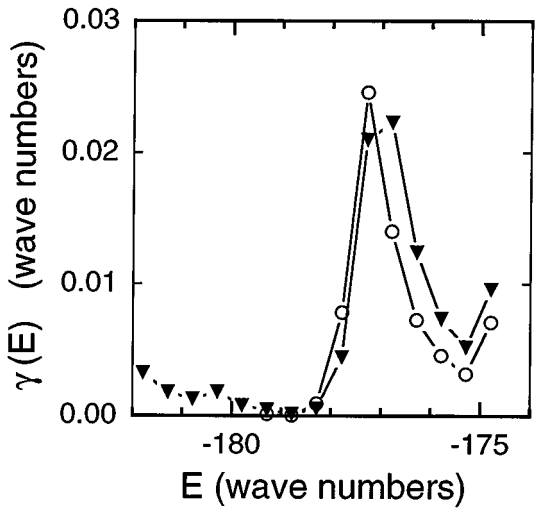

FIG. 11. $\gamma(E)$ versus E for the resonances between the $v=6$ quasibound ground van der Waals state with the $v=5$ continuum states. $\gamma(E)$ is large when one or more of the continuum states has significant amplitude in the region of the quasibound state. Just to the left of such a resonance, the Fano profile approaches zero. At that energy the lifetime of the quasibound state becomes very large because the $\Delta v=-1$ channel closes. Points represented with open circles are for a calculation which includes only $v=5$ channels in the basis of the continuum states. Points represented by solid triangles are for a calculation including $v=5$, 4, and 3 channels in the continuum basis.

respectively. The anomalously long lifetime and large fraction of $\Delta v=-2$ for $\alpha=1.8$ Å^{-1} are due to a degeneracy of the initial quasibound state with a long-lived resonance in the $\Delta v=-1$ manifold.

In order to understand the origin of the nonmonotonic behavior of the vibrational predissociation rate versus α, we have calculated the quantity

$$\gamma(E)=\pi\sum_{v,j}\ |\langle\psi_{j,v,E}|V(r,R,\theta)|\psi_{\text{bound},v=6}\rangle|^2,$$

where $\psi_{j,v,E}$ is the continuum wave function leading to $Ar+Cl_2(v,j)$ at total energy E and $\psi_{\text{bound},v=6}$ is the wave function describing the quasibound state of $ArCl_2$, $v=6$. $V(r,R,\theta)$ is the van der Waals interaction potential. Note that $\gamma(E)$ reduces to the golden rule approximation for the total line width of the quasibound $v=6$ level if E is equal to the energy of the quasibound state E_b. The goal here is to show that there are resonances in the $v-1$ continuum, and that they give rise to a nonexpected behavior of the linewidth as a function of α, because changing the value of α moves their positions. When there is a resonance in the continuum, the corresponding wave function has a significant probability density in the region of the well, hence (since $V(r,R,\theta)$ is a smoothly varying function) $\gamma(E)$ goes through a maximum. This can be seen in Fig. 11, where $\gamma(E)$ is plotted as a function of energy in the region of the quasibound $v=6$ state. However, the profile of this resonance is clearly asymmetric, going to zero on the lower energy side. This is due to the fact that there are two ways for the quasibound $v=6$ state to decay to the continuum: one is direct and the other one goes through the resonance. These two paths interfere; resulting in the Fano profile observed in Fig. 11. In particular, at the point where $\gamma(E)=0$, the $\Delta v=-1$ continuum is ''transparent'' and dissociation has to occur via direct $\Delta v=-2$ coupling, which is much slower.

This explains why vibrational predissociation from $v=6$ is so slow for $\alpha=1.8$ Å^{-1}. For that value of α, the Fano profile in the $\Delta v=-1$ continua has its zero very close to the energy of the quasibound state. Hence the $\Delta v=-2$ channel is strongly enhanced (18%) and the vibrational predissociation is quite slow. For other values of α, the position of the Fano profile is moved away from the quasibound state and the results go back to the more intuitive behavior given by the energy gap law. The Fano profile is due to a long lived resonance in the $\Delta v=-1$ channel; analogous to an orbiting resonance in scattering. To the extent that such a resonance were long lived, it could be thought of as a rotationally predissociative state. These resonances are most probable for cases in which the $\Delta v=-1$ channel is just barely open, such as described here. The fact that the calculated rotational distributions are a strong function of α is also explained by these resonances. The interferences between the quasibound state and the orbiting resonance have a sensitive dependence on α and this leads to the sensitivity of the rotational distribution on α. This effect should be smaller for the lower vibrational levels, and an experimental study of these levels would be useful for helping to determine the potential.

B. The $\Delta v=-2$ regime

In the $\Delta v=-2$ regime the fact that the calculated lifetimes and rotational distributions are quite sensitive to the assumed α parameter is not surprising since the dissociation dynamics depend on more or less coincidental degeneracies between the quasi-bound ''bright'' state and a ''dark'' state in the $\Delta v=-1$ manifold. The α parameter changes the strength of the coupling between the different vibrational manifolds, and also changes the density of states in each manifold. Smaller values of α correspond to a weaker coupling and a higher density of states. This can be seen in the $v=8$ spectra (Fig. 4): for $\alpha=1.6$ Å^{-1} the dark state resonances are spaced about 0.3 cm^{-1} apart in the region of the main resonance; while for $\alpha=1.8$ Å^{-1} the spacing is of the order of 0.5 cm^{-1}; and for $\alpha=2.0$ Å^{-1} the spacings are of the order of 1.0 cm^{-1}. For higher vibrational levels the dark state density goes down and the coupling goes up, for each value of α.

For the entire range of α values and vibrational levels considered here, IVR is best characterized as occurring in the sparse regime: The ''bright'' resonance mainly interacting with one or only a few dark resonances. This means that no monotonic trends can be expected for how the predissociation dynamics depends on v and α. Also, the range in values of observable properties is very large, for instance, the lifetime of the bright state varies from 24 ps to 19.4 ns. Not only is the range of values large, but the order is sometimes counter-intuitive. Increasing the coupling can cause the lifetime to increase! For instance, for $v=9$, the bright state lifetime for $\alpha=1.6$ Å^{-1} is 390 ps, while that for $\alpha=1.8$ Å^{-1} is 3.3 ns. This can be understood because for $\alpha=1.6$ Å^{-1} the spacing between the bright and the nearest dark state is only 0.17 cm^{-1}, while for $\alpha=1.8$ Å^{-1} the spacing is 0.57 cm^{-1}. Even for a single value of α, the calculated lifetime can vary by 2 orders of magnitude over the small range of vibrational levels. For $\alpha=1.6$ Å^{-1} the lifetime of the $v=8$ level is 19.4 ns, while that for $v=9$ level is 390 ps. That is, the two values are different by a factor of 50! For these resonances the spacings between the bright and dark states are about equal, so the difference in the lifetimes must be due to the detailed nature of the dark state. The lifetime of the dark state that couples with the $v=8$ bright state is only slightly longer than the one that couples to the $v=9$ bright state, so we conclude that this is not the major cause of the very different bright state lifetimes. Instead, the difference is mainly due to a poor overlap between the bright and dark state wave functions for $v=8$. Another indication that the mixing between the $v=8$ bright state and the strongest dark state is very small is that the integrated intensity of the dark state is very small, 0.05. Thus in the sparse limit of IVR the dissociation dynamics will be extremely sensitive to the spacings between the bright state and the nearest dark state, the specific nature of the dark state, and the coupling between these states.

An interesting example of the dependence of the coupling strength on the specific wave function of the dark state is provided by the $v=9$ calculations. In the top spectrum of Fig. 5, it is observed that there are three dark states on the high energy side of the bright state. The first of these dark states, *a*, is coupled very strongly, the second, *b*, quite weakly and the third, *c*, is coupled about twice as strongly as the second. This behavior can be explained by considering both the spacing of the resonances and the wave functions of the dark states as shown in Fig. 12. That the first dark state, *a*, is coupled strongly to the bright state is due to a combination of the fact that it is spaced only 0.15 cm^{-1} away from it and that its wave function has significant amplitude in the region of the bright state. The wave function for this resonance is shown in Fig. 12(a). It is seen that there is significant probability in the region between 3.9 and 4.1 Å perpendicular to the Cl–Cl axis where the bright state is localized. The second dark state is especially weakly coupled because its wave function, Fig. 12(b), has very little amplitude in the region of the bright state. The third dark state is coupled more strongly than the second, even though its energy is significantly more different from the bright state, because its wave function has higher amplitude in the region of the bright state wave function. This effect is repeated for $\alpha=1.8$ Å^{-1} as observed in the middle spectrum of Fig. 5 and the wave functions shown in Fig. 13. For this case the dark state that is within 0.6 cm^{-1} of the bright state, *a*, is only slightly more strongly coupled than the one that is 1.6 cm^{-1} away, *b*, because the overlap with the bright state wave function is much better for the dark state *b*, Fig. 13(b), than for dark state *a*, Fig. 13(a).

Since the goal of this study is to relate the dissociation dynamics of $ArCl_2$ to its potential energy surface, it is necessary to extract the underlying trends from the seemingly erratic dependence of the measurable properties on v and α. If we average over v, or α, some trends are evident. For instance, for $\alpha=1.6$ Å^{-1}, the average percent intensity in the dark state manifold is 8.8%; while for $\alpha=1.8$ Å^{-1} the average is 20% and for $\alpha=2.0$ Å^{-1} the average is 29%. From this it is apparent that the coupling increases with α faster than the density of states decreases. The measurable property that has the most direct dependence on α is the dissociation linewidth, Γ, which is inversely proportional to the bright state lifetime. In the case where the golden rule applies, Γ is proportional to the square of the coupling between vibrational manifolds. The average value of the square root of Γ for each value of α is 0.04, 0.12, and 0.19 $\text{cm}^{-1/2}$, for $\alpha=1.6$, 1.8, and 2.0 Å^{-1}, respectively. Similarly, averaging the square root of Γ over α gives the values 0.03, 0.09, 0.11, 0.13, and 0.22 $\text{cm}^{-1/2}$ for $v=8$, 9, 10, 11, and 12, respectively. Thus although the individual values of Γ do not have a monotonic dependence on v or α, the average values do. Therefore, if the lifetime is measured for many vibrational levels, this data could be used to estimate α for this potential.

In principle the product state distribution should contain considerable information about the intermolecular potential. Since the rotational distributions are very sensitive to both v and α, they serve as a very sensitive test for the potential. However, so far we have not been able to establish any trend that allows us to adjust the potential in order to obtain agreement between the measured and calculated distributions. The

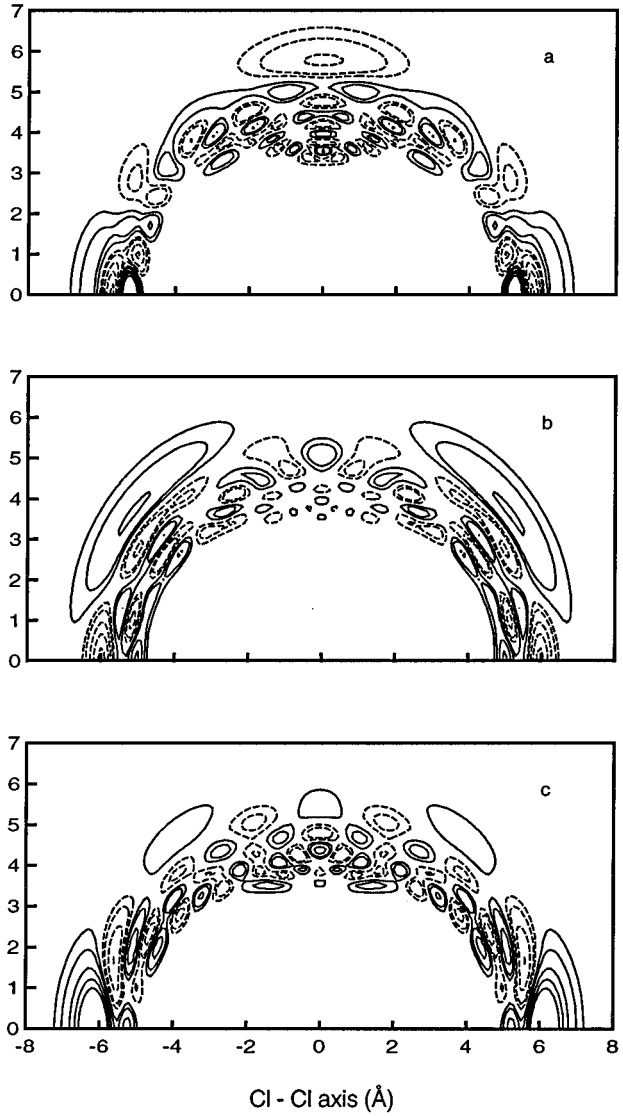

FIG. 12. $v=8$ wave functions for the dark states corresponding to the $v=9$ bright state, for $\alpha=1.6$ Å^{-1}. The states were obtained by diagonalization in an appropriate bend–stretch basis set and their energy was converged to better than 0.005 cm^{-1}. The top state, *a*, is the 47th even symmetry van der Waals excited state in the $v=8$ manifold (13.86 cm^{-1} below its dissociation limit). Its energy is -177.58 cm^{-1} with respect to the $v=9$ dissociation limit and hence it corresponds to the dark state resonance that is just to the right of the bright state in Fig. 5(a). The middle function, *b*, is the 48th even van der Waals excited state in the $v=8$ manifold. Its energy is -177.02 cm^{-1} with respect to the $v=9$ dissociation limit. The bottom function, *c*, is the 49th even van der Waals excited state in the $v=8$ manifold, at -176.68 cm^{-1} with respect to the $v=9$ dissociation limit. States *b* and *c* correspond to the second and third resonances to the right of the bright state in Fig. 5(a). Note that function *b* has significantly less amplitude in the region of $R(\mathrm{Ar–Cl_2})=3.9\pm0.2$ Å, perpendicular to the Cl_2 axis at the Cl_2 center of mass. This is the region of the bright state wave function. Since state a has good overlap with the bright state, and is also nearly at the same energy, it is strongly mixed and borrows significant intensity. Because the overlap between the bright state and function *b* is rather small, the corresponding transition is weaker than the transition to state *c*, even though state *b* is closer in energy to the bright state than is state *c*.

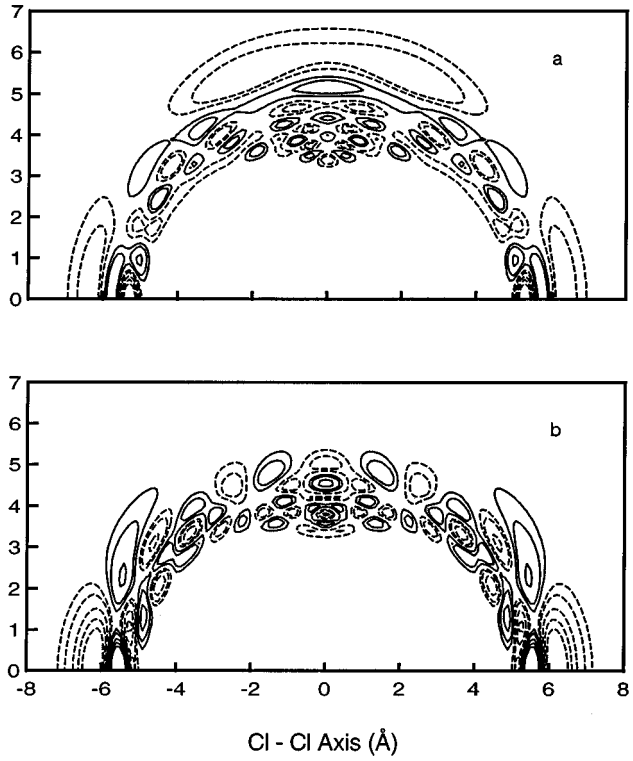

FIG. 13. $v=8$ wave functions for the dark states corresponding to the $v=9$ bright state, for $\alpha=1.8$ Å^{-1}. The states were obtained by diagonalization in an appropriate bend–stretch basis set and their energy was converged to better than 0.005 cm^{-1}. The upper plot, *a*, is the 43rd $v=8$ excited state at 13.228 cm^{-1} below the $v=8$ dissociation threshold, which corresponds to -176.947 cm^{-1} below the $v=9$ dissociation threshold hence to the first dark resonance to the right of the bright one in the middle spectrum of Fig. 9. The lower plot, *b*, is the 44th $v=8$ excited state at 12.239 cm^{-1} below the $v=8$ dissociation threshold which corresponds to -175.958 cm^{-1} below the $v=9$ dissociation threshold hence to the second dark resonance to the right of the bright one in the middle spectrum of Fig. 5(b). Notice that wave function *a* has little amplitude in the vicinity of $R(\mathrm{Ar–Cl_2})=4.0\pm0.1$ Å, perpendicular to the Cl–Cl axis, where the bright state has it's highest probability. In contrast, function *b* has a peak in its probability in this region. This accounts for the fact that the two functions are about equally coupled to the bright state even though function *a* is much closer in energy to the bright state than is function *b*.

percent of vibrational predissociation that occurs through the $\Delta v=-2$ channel varies smoothly with α, and may be measurable for the higher vibrational levels. In the experimental study of $ArCl_2$ predissociation,[1] it was noted that the $\Delta v=-3$ channel was never observed even for $v=12$. Although no sensitivity analysis was given, probably this implies that $\Delta v=-3$ dissociation accounts for less than 5% of the total. This would imply that the true value of α is towards the lower end of the range tested here. This conclusion is also supported by the experimental measurement that the lifetime for the $v=11$ level is longer than 85 ps.

It is encouraging to note that the average fraction of the available kinetic energy that goes into rotation is quite similar for the experimental measurements[1] and the calculations reported here. For both the experiment and the calculation, there was no obvious trend in how this fraction depends on the initial vibrational quantum number. For the experiment, this fraction ranges from 24% to 35%, with an average value of 30%. For the calculations using $\alpha=1.8$ Å^{-1}, the fraction ranges from 15% to 44%, with an average value of 32%. For $\alpha=1.6$ Å^{-1} the average rotational energy is considerably higher than measured for each vibrational level. This implies

that the true value of α is higher than 1.6 $Å^{-1}$. Combined with the conclusion of the previous paragraph, our initial estimate for α, 1.8 $Å^{-1}$, appears to be quite reasonable. We conclude that $\alpha = 1.8 \pm 0.1$ $Å^{-1}$. In the future, it would be very useful to accurately measure both the lifetimes and the vibrational distributions to more accurately determine the α parameter. The rotational distributions could then be used to adjust the anisotropy of the potential.

V. SUMMARY

In this study we have examined both the direct dissociation regime ($\Delta v = -1$) and the IVR regime ($\Delta v = -2$) for the vibrational predissociation of $ArCl_2$. In particular, we explored the dependence of the dissociation dynamics on the value used for the Morse range parameter, α. The direct dissociation regime was found to be much more complicated than expected due to mixing between the quasibound states and resonances in the dissociation continuum. These resonances probably correspond to high orbital angular momentum states in which the Ar is trapped behind the centrifugal barrier. Because the total angular momentum is zero for all of these calculations, another description of the same behavior would be to say that the continuum state corresponds to a rotationally predissociative state. In this language, the $\Delta v = -1$ process could also be thought of as IVR in the sparse regime. In any case, the result is that the predissociation rate is very sensitive to the value assumed for α. For example, in the region of such a resonance a ten percent change in the value assumed for α can result in a 2 order of magnitude change in the dissociation rate. Unfortunately, this complicated behavior will make it difficult to determine the potential energy surface for $ArCl_2$. This difficulty could be partially overcome if the propensity for the $\Delta v = -2$ dissociation could be measured to help determine the magnitude of the coupling to the continuum resonances. Another way to avoid this problem would be to study lower vibrational levels.

The behavior of the dynamics in the IVR regime is also quite complicated due to the fact that the dynamics are controlled by both the energy and the detailed wave function of the doorway state that happens to be in resonance with any given bright state. Again, the lifetime of a bright state can change by 2 orders of magnitude with a ten percent change in the assumed value of α. However, if the calculated lifetimes are averaged over several vibrational levels, then the dependence of this average on the value assumed for α is about as expected. We conclude that measurement of such a series of lifetimes would be the most useful data for the next step in the determination of the potential. Based on the small amount of data currently available for the lifetimes and the $\Delta v = -2$ propensity in the $\Delta v = -1$ regime, we believe that the correct value of α is in the middle of the range explored here, or about 1.8 $Å^{-1}$.

Although the full scattering calculations presented here are necessary for a quantitative comparison with data, it was found that golden rule calculations are accurate enough that they may be used for a rough fit of the potential. This will be very helpful since the golden rule calculations are many orders of magnitude faster than the spectrum calculations.

ACKNOWLEDGMENTS

This work was supported by the United States National Science Foundation CHE-9423504. In addition, K.C.J. and N.H. wish to acknowledge the joint NSF-CNRS collaboration program for the support of international travel that made this work possible. The calculations were performed on the Convex c3840 Computer supported by the School of Physical Sciences and the Office of Academic Computing at the University of California, Irvine. We would like to thank Professor J. A. Beswick for many helpful discussions during the course of this study, and Professor V. A. Apkarian for discussions regarding the potential energy surfaces.

[1] D. D. Evard, C. R. Bieler, J. I. Cline, N. Sivakumar, and K. C. Janda, J. Chem. Phys. **89**, 2829 (1988).
[2] N. Halberstadt, J. A. Beswick, O. Roncero, and K. C. Janda, J. Chem. Phys. **96**, 2404 (1992); N. Halberstadt, S. Serna, O. Roncero, and K. C. Janda, *ibid*. **97**, 341 (1992).
[3] J. I. Cline, B. P. Reid, D. D. Evard, N. Sivakumar, N. Halberstadt, and K. C. Janda, J. Chem. Phys. **89**, 3535 (1988).
[4] J. I. Cline, N. Sivakumar, D. D. Evard, C. R. Bieler, B. P. Reid, N. Halberstadt, S. R. Hair, and K. C. Janda, J. Chem. Phys. **90**, 2605 (1989); N. Halberstadt, J. A. Beswick, and K. C. Janda, *ibid.* **87**, 3966 (1987).
[5] O. Roncero, P. Villareal, G. Delgado-Barrio, N. Halberstadt, and K. C. Janda, J. Chem. Phys. **99**, 1035 (1993).
[6] S. K. Gray and O. Roncero, J. Phys. Chem. **99**, 2512 (1995).
[7] S. K. Gray and O. Roncero, J. Chem. Phys. **104**, 4999 (1996).
[8] M. L. Burke and W. Klemperer, J. Chem. Phys. **98**, 1797, (1993).
[9] D. D. Evard, J. I. Cline, and K. C. Janda, J. Chem. Phys. **88**, 5433 (1988).
[10] Y. J. Xu, W. Jager, I. Ozier, and M. C. L. Gerry, J. Chem. Phys. **98**, 3726 (1993).
[11] F.-M. Tao and W. Klemperer, J. Chem. Phys. **97**, 440, (1992).
[12] J. Sadlej, G. Chalasinski, and M. M. Szczesniak, J. Chem. Phys. **99**, 3700 (1993).
[13] J. A. Beswick and J. Jortner, Adv. Chem Phys. **47**, 363 (1981).
[14] R. L. Waterland, M. I. Lester, and N. Halberstadt, J. Chem. Phys. **92**, 4261 (1990).
[15] O. Roncero, J. A. Beswick, N. Halberstadt, P. Villarreal, and G. Delgado-Barrio, J. Chem. Phys. **92**, 3348 (1990).
[16] Here the correlation coefficient is defined as $\Sigma_j P_{j,BS} P_{j,DS} \div \Sigma_j P_{j,BS}^2$, where $P_{j,BS}$ is the probability that the Cl_2 fragment was in level j upon dissociation via a bright state resonance and $P_{j,DS}$ is the probability that the Cl_2 fragment was in level j after dissociation via the associated dark state resonance.